Modeling of the heat transfer process in an air heat pump fanless evaporator

Piotr Kopeć[1,*], *Beata* Niezgoda-Żelasko[2]

[1,2] Institute for Thermal and Process Engineering, Cracow University of Technology, al. Jana Pawła II 37, 31-864 Cracow

Abstract. This paper analyses the mixed convection process in a fanless evaporator of an air heat pump. The text of the paper shows the authors' experimental studies results of the temperature distribution and the local values of heat transfer coefficients on the outer surface of vertical tubes with longitudinal fins for the case of mixed convection and fins of a specific shape of their cross-section (prismatic, wavy fins). The experimental studies include the air velocities w_a=2,3 m/s and the temperature differences between air and the refrigerant inside the heat exchanger tubes which is ΔT=24-40K. The results obtained were used for verification of CFD modeling of the heat transfer process for the discussed case of heat transfer and the geometry of the finned surface. The numerical analysis was performed for: the temperature distribution along the fin height, the tube perimeter and height, the distribution of local heat transfer coefficients on the finned tube perimeter and along its height. The simulated calculations were used to verify the method of determination of fin efficiency.

1 Introduction

Air is one of the types of bottom heat sources for heat pumps. The structure/design of an evaporator depends on the media involved in the heat transfer process and the manner air is obtained (natural or forced convection). In air heat pumps we can distinguish evaporators with forced air flow (fan exchangers) and fanless ones, working in conditions of free (natural) convection or mixed convection. A fanless evaporator is fabricated as a freely arranged system of vertical longitudinally-finned tubes [1]. The applicability of equations which may be used to calculate the air-side heat transfer coefficients depends on the flow type and geometry. For instance, the equations used for horizontal lamellated or transversely finned tubes include those proposed by: Schmidt [2], Norris-Spoford [3], Stasiulevicius [4] and Briggs-Young [5]. Papers [6] and [7] present the methods of measurements of local and mean heat transfer coefficients during transverse airflow around horizontal membrane tubes or tubes with two ribs (fins) under forced convection conditions. The authors of papers [8] and [9] looked at the heat transfer processes during forced transverse flow of exhaust gas around a horizontal bank of tubes with three ribs (fins).

The numerical analysis of natural convective heat transfer processes in natural convection processes on the surface of longitudinal fins is often performed for the flow inside longitudinally-finned tubes [10], [11]. Modeling of a heat transfer process can be used to solve reverse issues, in order to determine local mean heat transfer coefficients on membrane surfaces, after adopting the experimental study results as boundary conditions in solution of a system of equations of conservation (of momentum, energy, mass) [13]. The methods of this type are also used to search for solutions which will maximize the heat transfer coefficient [14], [15]. Experimental determination of mean or local values of heat transfer coefficients, especially for finned surfaces, is a complex measurement problem. This paper presents the heat transfer modeling process for fanless evaporators operated in the mixed convection conditions.

2 Experimental Studies

This paper presents the studies of heat transfer from the side of the bottom source of heat in a fanless evaporator of an air heat pump. The evaporator is made of vertical bimetallic tubes. The core of the evaporator tube is a copper tube. The outer part is an aluminium tube with drawn longitudinal fins having a specific shape, arranged centrally symmetrically along the circumference of the tube (see Figure 1). As the heat exchanger is operated in variable external conditions, the evaporators of that type can work in natural convection conditions and mixed convection conditions at low flow velocities (rates) and longitudinal or transverse flow around the tubes of the evaporator.

The experimental setup consisted of a system of two vertical finned tubes of the height of 2 m, whose axes were located at the distance of S_q=0.2306 m from each other. The experiments were carried out in a horizontal channel with a 2x0.464 m rectangular flow cross-section and the length of L_p=2.5 m (Figure 2). Airflow in the channel was forced using a radial fan. The heat exchanger tubes were fed with ice water at the

* Corresponding author: piotr.kopec@mech.pk.edu.pl

temperature of 7˚C or with refrigerants (R407C and R507), having evaporation temperatures of: $-25 \leq T_R \leq -5$ (˚C).

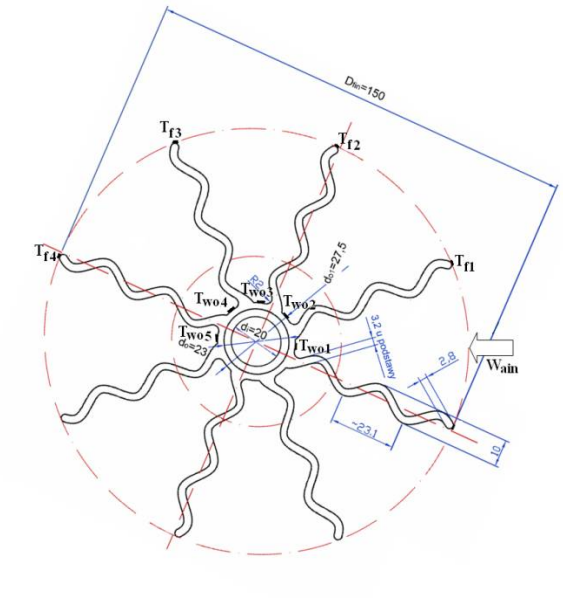

Fig. 1. Bimetallic tube cross-section.

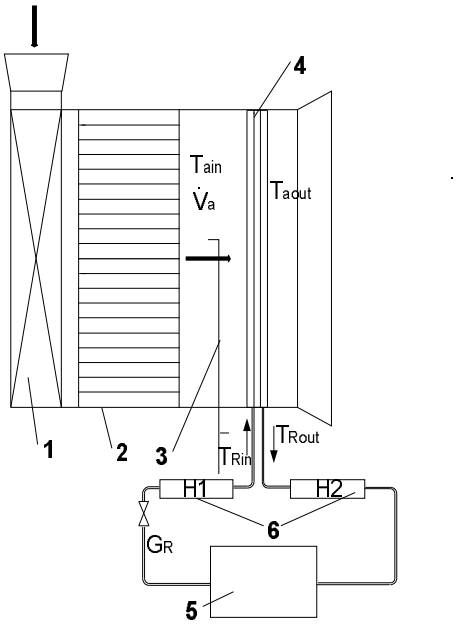

Fig. 2. Experimental setup: 1-radial fan, 2-flow stream equalizer, 3- Pitot tube, 4-studied tubes, 5-condensing unit, 6-electric heaters.

Calibrated NiCr-NiAl thermocouples were placed on the outer surface of one of the tubes to enable the measurement of the temperature of the outer tube surface and of the fin tips in the upper and lower part of the exchanger (Figure 1). The heat flux transferred from the air to the heat transfer surface was calculated using the heat balance equation for the cooling medium (water or refrigerant) [12].

2.1 Experimental studies results

During the experimental studies at the mentioned setup the temperature was measured of both bases and ends (tips) of the fins, in the top and bottom parts of the tube. The bottom means the measurement at the distance of 20 cm from the tube base, the top means the location at the distance of 170 cm from the tube base. On the basis of the data obtained, corresponding to the mixed convection conditions, the distribution of temperatures on the fin surface was determined.

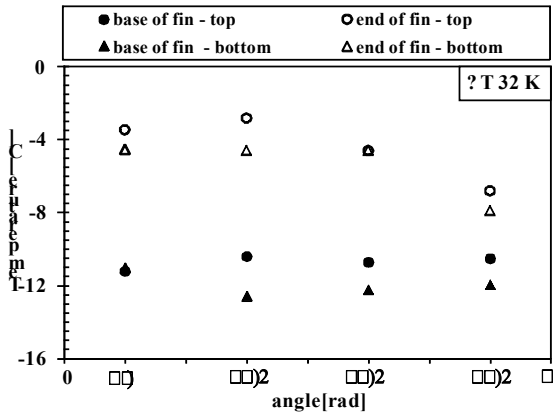

Fig. 3. Example of temperature distributions for mixed convection, ΔT=32K, w_a=2,3 m/s.

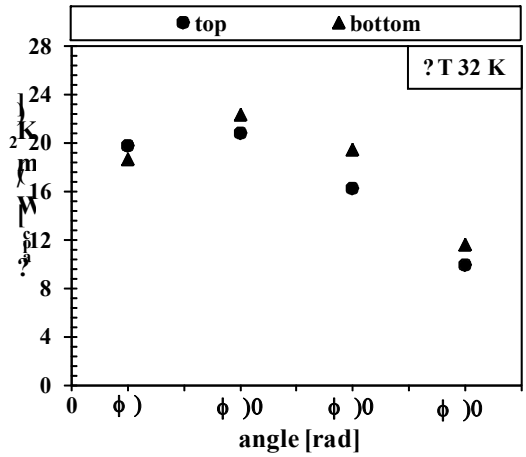

Fig. 4. Example of values of local heat transfer coefficients for mixed convection, ΔT=32K, w_a=2.3 m/s.

Figure 3 shows an example of temperature distributions on the surface of one tube of the air heat pump evaporator, operated in the mixed convention conditions.
Then these values were used to determine the values of the air-side heat transfer coefficients. In order to do that, the method of determining the local values of coefficients was used, as presented in the paper by Niezgoda-Żelasko, Żelasko [12]. Figure 4 shows an example of values of local heat transfer coefficients corresponding with the temperatures distribution shown in Figure 3.

3 Numerical modelling of the heat transfer process

The heat transfer process between the finned tube and external air was modeled using the finite volume method and Ansys-Fluent software. The forced convection process modelling, the shape of the fins of the exchanger and the transverse direction of airflow required the modeling to be carried out in a 3D space. Due to the occurrence of the frontal surface (of inflow), the individual fins work in different ambient conditions. In this case the model could not be limited to one fin. An even number of fins in the exchanger allowed to assume a vertical symmetry axis and make a half of a real model. Air was modeled as a perfect incompressible gas. The dynamic viscosity coefficient and other physical parameters were assumed as constant values. Gravitational force was assumed along the model vertical axis. The mixed convection process modeling was carried out assuming the condition of the frontal velocity in the direction transverse to the exchanger under examination, the gravitational force being taken into account.

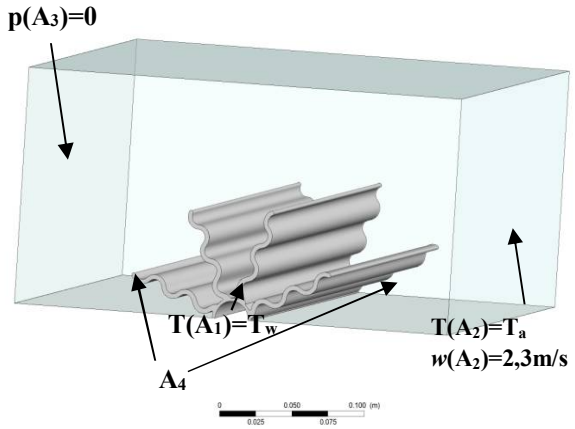

Fig. 5. The model and the boundary conditions.

The turbulent air flow was assumed and the k-ω SST turbulence model was adopted. This model combines the features of the model k-ε, and the model k-ω. The model k-ω is more adequate for solving problems in the boundary layer, while the model k-ε better describes turbulent flow.

The following boundary conditions were assumed as presented in Figure 5:

- constant temperature of the inner fin surface: $T(A_1)=T_w$,
- constant air temperature at the inlet: $T(A_2)= T_a$,
- condition of constant pressure at the air outlet $p(A_3)=0$,
- condition of velocity at the inlet $w(A_2)=2.3$ m/s,
- condition of symmetry for surface A_4,

The evaporator geometrics model was performed for real dimensions of the examined exchanger. Due to large dimensions of the exchanger, the number of elements of the calculation grid generated exceeded $9 \cdot 10^6$. The grid was hexagonal. In the areas of overlapping of the boundary conditions and in the area of air contact with the exchanger, the grid was refined. The thermodynamical parameters to be taken into consideration in the calculation model of the Fluent software corresponded to the operation parameters of the exchanger in real-life conditions.

3.1. Numerical analysis

The numerical analysis concerned the temperature distribution along the height of a fin for individual fins fixed on the perimeter of the exchanger tube as in Figure 1. CFD simulation was performed for the same heat transfer conditions and the temperature distribution along the studied fin was determined. The simulations were carried out for various values of the exchanger inner wall temperature.

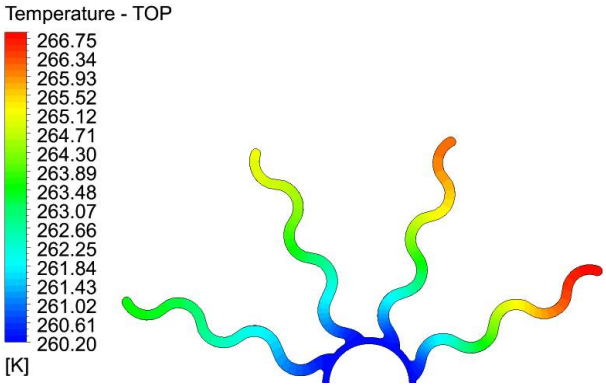

Fig. 6. Temperature distribution for CFD calculations, for mixed convection, ΔT=32K, w_a=2.3 m/s – top of the fin.

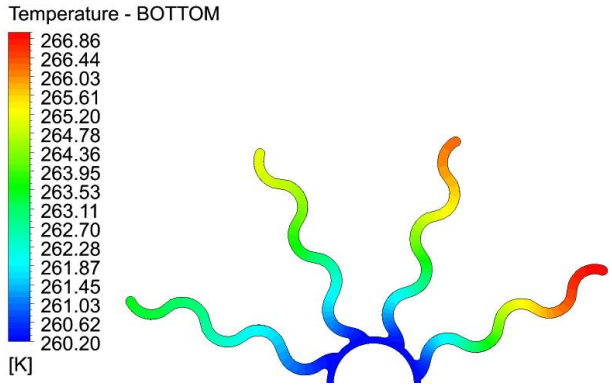

Fig. 7. Temperature distribution for CFD calculations, for mixed convection, ΔT=32K, w_a=2.3 m/s – bottom of the fin.

Figure 6 and 7 shows the temperature distribution in top and bottom parts of a fin, as obtained from the CFD modelling process. Figure 8 presents a comparison of the temperature values obtained at the base of fin and end of fin in its bottom and top parts, obtained from measurements and simulations. The direction of airflow and location of the fins in relation to it results in the difference of the temperature distribution for individual fins. This is confirmed by the temperature values obtained at the base and at the end of a fin, Figure 8.

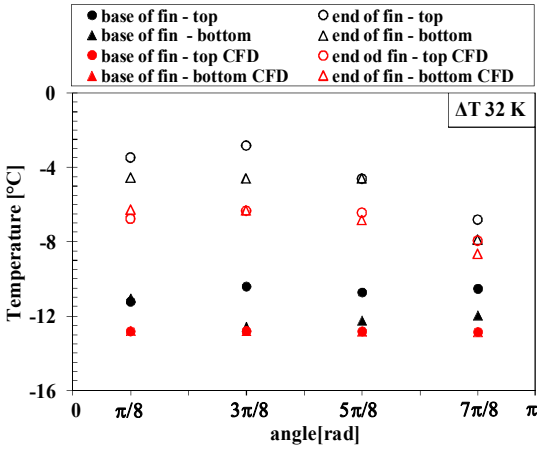

Fig. 8. Temperature distribution for CFD calculations, for mixed convection, ΔT=32K, w_a=2.3 m/s.

The second fin achieves the highest temperature – angle 3/8π. The maximum temperature value on the second fin results from the fact that it is almost perpendicular to inflowing air direction and consequently it is lipped by the largest stream of air volume. The results presented in Figure 8 evidence that in each of the cases discussed the qualitative distribution of temperature for measurements and simulation is similar. Various temperature values T_w will affect local values of heat transfer coefficients. Lower values T_w increase the temperature difference between ambient air and temperature T_w, which affects the higher values of heat transfer coefficients. Figure 9 presents an example of comparison of the local heat transfer coefficient values obtained.

The local heat transfer coefficients obtained by CFD modeling have similar values to the coefficients determined from experimental data.

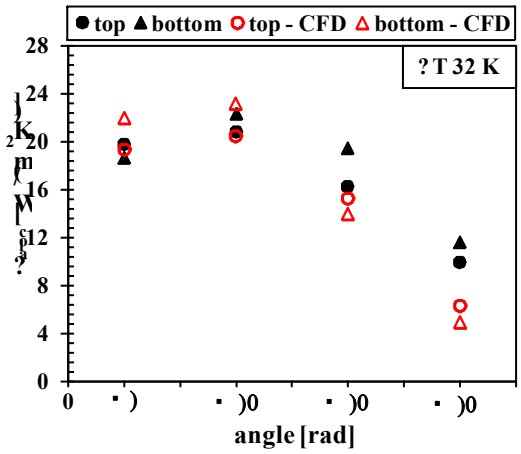

Fig. 9. Example of local heat transfer coefficient values obtained from CFD modeling for mixed convection, ΔT=32K, w_a=2.3 m/s.

The nature of changes in the coefficients is the same. The change of coefficients complies with the change in the fin temperature value. The highest local values are for the second fin, then for the first fin. These fins are situated on the side of the air inflow. In this area the air velocities are the highest, which determines the local heat transfer coefficients values.

3.1.1 Fin efficiency determination

The experimental studies and simulation calculations allowed to verify Schmidt's equations (1) for determination of fin efficiency. In the case of the discussed fin, the fin height "S" corresponds to the height of a straight fin having the surface area equivalent to the studied fin area. The temperature distribution obtained from experiment and from CFD modeling allowed to determine the verification efficiency of a fin from equation (2). Sample results of calculations for top and bottom of a fin are listed in Table 1.

$$\varepsilon_{fin-S} = \frac{\tanh(Sm)}{Sm} \quad (1)$$

$$\varepsilon_{fin} = \frac{\overline{T}_{fin} - T_a}{\overline{T}_w - T_a} \quad (2)$$

In mixed convection conditions individual fins feature various efficiencies, but not lower than 84%. The highest efficiencies for a given temperature difference between an internal surface of a heat exchanger and air are achieved by fins located on the leeward side, exceeding 91%. The discrepancies between the values obtained from simulation and the experimental parameters do not exceed 6%.

Table 1. Comparison of fins efficiencies.

ΔT=32K	Fin top			
angle	π/8	π3/8	π5/8	π7/8
ε_{fin-S} – (1)	0,874	0,874	0,874	0,874
$\varepsilon_{fin-exp}$– (2)	0,847	0,847	0,875	0,924
ε_{fin} – CFD	0,896	0,889	0,889	0,916

ΔT=32K	Fin bottom			
angle	π/8	π3/8	π5/8	π7/8
ε_{fin-S} – (1)	0,865	0,865	0,865	0,865
$\varepsilon_{fin-exp}$– (2)	0,847	0,847	0,863	0,919
ε_{fin} – CFD	0,880	0,860	0,909	0,964

4 Conclusions

The paper discussed an analysis of the heat transfer process in a fanless evaporator of an air heat pump. The temperature distribution on the outer surface of longitudinally finned tubes was analysed. The results obtained from experimental studies were compared to the temperature distribution obtained from numerical modeling of the heat transfer process, using finite volume method (Fluent). The discrepancies between the values obtained are minute. The relative difference of the measured and calculated temperatures along fin height was smaller than 2%.

The lowest temperature value of a fin end can be observed on the last fin – fixing angle 7/8π. This fin is located leeward. It is obstructed by preceding fins which consequently hinder its direct contact with the airflow. Additionally, the pressure is lower in this area. It results in air whirls and inflow of air of lower temperature, which is cooled down earlier by preceding fins. It should also be noted that the fin temperatures at the bottom of the exchanger are lower than the temperatures in its top part. This difference may result from the buoyant forces affecting the heat transfer process. The air giving up energy gets its temperature lower and increases its density. Apart from the air inflow, there is also an additional vertical airflow connected with the presence of buoyant force and whirls in the inter-fin area.

Using the temperature distribution, a comparison of fin efficiency calculation methods was carried out. The results obtained on the basis of these methods feature similar values and relative differences between the measured and calculated fin efficiencies do not exceed 4%.

Nomenclature

$\dot{G}$	refrigerant mass stream density, (kg/(m^{2}s))
S	substitute height of a straight fin having the area of a real fin, $S = A_{fin} / \left(n_{fin} \cdot L\right)$, (m)
S_q	tube spacing, (m)
s	fin thickness, (m)
m	parameter in formula (1) $m = \sqrt{(2 \cdot RCJ \cdot \alpha_{loc} / (s \cdot \lambda_{fin})}$, (1/m)
n	number of fins, (-)
L_p	channel length, (m)
RCJ	degree of process openness [16], (-)
T	temperature, (˚C)
w	velocity, (m/s)

Symbols

Δ	increment
α	heat transfer coefficient, (W/(m^{2}K))
ε	fin efficiency, (-)
ϕ	measurement channel diameter, (m)
λ	thermal conduction coefficient, (W/(mK))

Subscripts

a	air
f	fin tip
fin	fin
loc	local value
R	refrigerant (cooling agent or water)
w	wall

References

1. B. Niezgoda-Żelasko, W. Zalewski, J. Żelasko, *Experimental research of the air-water heat pump with evaporator operating under free convection conditions* (Proceedings from the 44th Science and Technology Conference - Refrigerations Days, Poznań)
2. VDI-Wärmeatlas, 1991, Wärmeübertragung bei Querströmung um einzelne Rohrreihen und durch Rohrbündel, Gf 1- Gf 3, (Düsseldorf :VDI Verlag).
3. L. Kołodziejczyk, M. Rubik, *Refrigeration and air conditioning technology* (Warszawa: Arkady, 1976) (in Polish)
4. J. Stasiulevisius, V. Survila, Paper FC 6.5. Proc. 5th Int. Heat Trans. Conference, Tokyo (1974)
5. D. E. Briggs, E. H. Young, Chemical Engineering Programming Symposium, Ser. **59**. (1963)
6. J. Taler, T. Sobota, A. Cebula, Arch. of Therm. **26,** 1, pp 35-52 (2005)
7. J. Taler, A. Cebula, Mechanika, **202**, pp. 263-272 (2003)
8. M. Pronobis, S. Kalisz, R. Wejkowski, Heat and Mass Trans., **38,** pp. 343–350 (2002)
9. R. Wejkowski, M. Pronobis, *New kinds of convective tube bank - a comparison of physical and numerical modeling of heat transfer and pressure loss,* (Int. Conference: Combustion and Environment, Ostrava, Czech Republic, 2003)
10. I. M. Rustum, H. M. Soliman, Int. J. Heat Mass Trans., **33,** 7, pp. 343–350 (1990)
11. J. C. Chai, S. V. Patankar, Num. Heat Trans., **Part A 24,** pp. 67-87 (1993)
12. B. Niezgoda-Żelasko, J. Żelasko, Exp. Therm. And Fluid Sci., **57,** pp. 145-156 (2014)
13. J. Taler, T. Sobota, A. Cebula, Arch. of Therm., **26** 1, pp. 35-52 (2005)
14. S.C. Haldar, Int. J. of Therm. Sci., **49,** pp. 1977-1983 (2010)
15. A. Kumar, J. B. Joshi, A. K. Nayak, P.K. Vijayan, Int. J. of Heat and Mass Trans., **92,** pp. 507-522 (2016)
16. B. Niezgoda-Żelasko, W. Zalewski, *Refrigeration and air conditioning heat exchangers: thermal calculations* (Kraków, 2012) (in Polish)